A semiquantitative analysis of reactive astrogliosis demonstrates its correlation with the number of intact motor neurons after transient spinal cord ischemia

Satoru Wakasa, MD, PhD, Norihiko Shiiya, MD, PhD, Tsuyoshi Tachibana, MD, PhD, Tomonori Ooka, MD, PhD, and Yoshiro Matsui, MD, PhD

Objective: We evaluated the relationship between reactive astrogliosis and delayed motor neuron death after transient spinal cord ischemia in rabbits using a semiquantitative analysis of glial fibrillary acidic protein expression.

Methods: Spinal cord ischemia was induced by means of balloon occlusion of the infrarenal aorta for 15 minutes at 39°C in 18 New Zealand white rabbits. At 1, 3, and 7 days after reperfusion, 6 animals at each time point were killed, and the spinal cord was removed for histologic and immunohistochemical study. The variables analyzed were (1) neurologic function (Johnson score) at every 24 hours after reperfusion, (2) the number of intact motor neurons and terminal deoxynucleotidyl transferase–mediated deoxyuridine triphosphate-biotin nick-end labeling–positive positive neurons, and (3) expression of glial fibrillary acidic protein in the gray and white matter, which was expressed as the percentage of stained area.

Results: All animals presented delayed motor neuron death. The number of intact neurons decreased correlatively with neurologic function. No obvious terminal deoxynucleotidyl transferase–mediated deoxyuridine triphosphate-biotin nick-end labeling–positive cells were observed. Glial fibrillary acidic protein expression increased with time in both the gray and white matter, representing the development of reactive astrogliosis. Significant correlation was found between glial fibrillary acidic protein expression and the number of intact motor neurons on the third day in both the gray ($r^2 = 0.726$, $P = .031$) and white ($r^2 = 0.927$, $P = .002$) matter.

Conclusions: Reactive astrogliosis 3 days after transient spinal cord ischemia correlates with the number of intact motor neurons. Our method for semiquantitative analysis of reactive astrogliosis is simple and reproducible and seems useful for such experimental studies.

Preventing paraplegia after thoracoabdominal aortic surgery remains a challenging problem. Postoperative spinal cord damage develops in 2 different time periods. Immediate neurologic deficits are noted at emergence from anesthesia, whereas delayed deficits affect patients with initially intact neurologic function.[1] Delayed onset or progression of motor neuron death was also reported in animal models 2 to 7 days after transient spinal cord ischemia (TSCI).[2-8] The mechanism of this ''delayed'' motor neuron death still remains controversial. Although apoptosis is considered one of the most likely causes,[3-5] necrotic death is also suggested to be predominant in delayed neuronal death,[7] and astrocytes could play a crucial role.[8]

Many functions of astrocytes are considered to be important in determining the tissue response to ischemia or trauma of the central nervous system, including their role in the control of fluid movements between the intracellular and extracellular spaces, the ability to take up glutamate and reduce excitotoxicity, and their role in spatial buffering.[9] After brain ischemia and reperfusion, astrocytes are activated (reactive astrocytes) with upregulated expression of glial fibrillary acidic protein (GFAP), resulting in ''reactive astrogliosis.'' Reactive astrocytes might either reduce or exacerbate the damage to neurons depending on the time point or postischemic stage.[10] Indeed, in the ischemic penumbra reactive astrogliosis is considered to be associated with delayed infarct expansion after permanent or transient occlusion of the middle cerebral artery in rats.[11,12] Therefore we hypothesized that reactive astrocytes could also play an important role in delayed neuron death in the spinal cord.

In the spinal cord, however, studies demonstrating the relationship between astrocytes and ischemic, especially delayed, motor neuron death are sparse. In addition, the development of astrogliosis has usually been evaluated by using histologic grading methods, and semiquantitative analysis of correlation between motor neuron death and reactive astrogliosis has not thus far been reported. The purpose of this study is to establish an experimental method that allows semiquantitative analysis of astrocyte activation and to investigate the correlation between delayed motor neuron death and development of reactive astrogliosis by using this model.

From the Department of Cardiovascular Surgery, Hokkaido University Hospital, Sapporo, Japan.

Received for publication June 16, 2008; revisions received Aug 27, 2008; accepted for publication Oct 3, 2008.

Address for reprints: Satoru Wakasa, MD, PhD, Department of Cardiovascular Surgery, Hokkaido University Hospital, Kita-14, Nishi-5, Kita-ku, Sapporo 060-8648, Japan (E-mail: wakasa@med.hokudai.ac.jp).

J Thorac Cardiovasc Surg 2009;137:983-90
0022-5223/$36.00

doi:10.1016/j.jtcvs.2008.10.002

Abbreviations and Acronyms

GFAP = glial fibrillary acidic protein
GFAP% = GFAP-positive area fraction
TSCI = transient spinal cord ischemia
TUNEL = terminal deoxynucleotidyl transferase–mediated deoxyuridine triphosphate-biotin nick-end labeling

MATERIALS AND METHODS

The experimental protocol was approved by the Ethics Committee for Animal Experimentation at Hokkaido University School of Medicine. Eighteen New Zealand white rabbits weighing 3.10 ± 0.04 kg (range, 2.80–3.50 kg) were used in this study.

Surgical Procedure

Anesthesia was induced with intramuscular administration of ketamine at a dose of 50 mg/kg and maintained with inhalation through a face mask of 2% to 4% isoflurane driven by 1 L/min oxygen. The animals were allowed to breathe spontaneously. Body temperature was continuously monitored with a rectal thermistor and was maintained at 39°C with the aid of a heating pad (Asahi Plate Warmer TK-43; Asahi Denshi, Inc, Osaka, Japan) during the procedure. A 24-gauge intravenous catheter was placed in the marginal ear vein for administration of fluid and drugs. Acetated Ringer's solution with 25 mEq/L sodium bicarbonate was infused at a rate of 10 mL · kg^{-1} · h^{-1}. The proximal arterial blood pressure was monitored continuously through a 24-gauge intra-arterial catheter placed in the median ear artery. Intravenous cefazolin (30 mg/kg) was administered before the incision was made. The rabbits were placed in the supine position, and a small skin incision was made at the right groin. The right femoral artery was exposed and dissected. After intravenous administration of heparin sodium (100 IU/kg), a 4F angiographic balloon catheter (CI-304; Harmac Medical Products, Inc, Buffalo, NY) was inserted through the artery and advanced 15 cm cephalad into the abdominal aorta. Our previous study confirmed that the balloon at the tip of the catheter inserted to such a distance was positioned just caudal to the left renal artery.[13] After stabilization of blood pressure and rectal temperature, TSCI was induced by means of balloon aortic occlusion for 15 minutes. Definitive occlusion was confirmed by the loss of pulse pressure on the distal blood pressure monitor, which was measured through the side hole of the catheter. Arterial blood gas analyses were performed at 5 minutes before and after the ischemic period. At the end of the operation, catheters were removed, the surgical wound was closed, and the rabbits were allowed to recover at ambient temperature and were returned to their cages.

Experimental Protocol

The animals were killed after achievement of deep anesthesia with intravenous administration of sodium pentobarbital (50 mg/kg) immediately after neurologic testing on the first, third, and seventh days after reperfusion (n = 6 each, the first day means the day after the operation). After death, the lumbosacral portion of the vertebrae was taken out en bloc, and the spinal cord was removed carefully and quickly. Thereafter, the L4 to L5 segments were dissected in 3 or 4 pieces. Some of those blocks for histologic study were fixed by means of immersion in 10% formalin solution and embedded in paraffin. The rest of the blocks were frozen in liquid nitrogen with Tissue-Tek O.C.T. compound (4582; Sakura Finetechnical Co, Ltd, Tokyo, Japan) and stored at –80°C for immunohistochemical analysis.

Neurologic Assessment

The rabbits' hind-limb function was evaluated at every 24 hours after reperfusion, according to the method of Johnson and colleagues[14] on the following 6-grade scale: 0, hind-limb paralysis; 1, severe paraparesis; 2, functional movement with no hop; 3, ataxia with disconjugate hop; 4, minimal ataxia; and 5, normal function. An observer unaware of the protocol assessed neurologic function.

Histologic Study

Serial transverse sections (4 μm) were obtained and stained with hematoxylin and eosin for histopathologic study. Terminal deoxynucleotidyl transferase–mediated deoxyuridine triphosphate-biotin nick-end labeling (TUNEL) staining was also performed with a detection kit (298-60201, Apoptosis In Situ Detection Kit; Wako, Osaka, Japan) to detect apoptotic neuronal death. The reliability of the TUNEL staining method was validated by staining the positive control samples, which were created from 2 control animals without spinal cord ischemia by means of pretreatment with DNase-I. All sections were evaluated at a magnification of ×200.

In hematoxylin and eosin staining intact neurons in the anterior spinal cord were counted in each slice. We defined apoptotic and necrotic neurons as follows. Neurons presenting cytoplasmic shrinkage, nuclear chromatin condensation (crescentic or round), and apoptotic bodies were considered apoptotic. Neurons with loss of Nissl bodies, cytoplasmic vacuolization, structureless cytoplasm (sometimes with findings of cell lysis), and degeneration of nuclei were considered necrotic. Mildly damaged neurons with swelling and dispersed Nissl substances were counted as intact neurons in this study. Counted data from 3 different slices in each animal were averaged and compared. In TUNEL staining apoptotic neurons were defined as the nucleus stained dark brown with or without chromatin condensation and apoptotic bodies in association with translucent cytoplasm, whereas necrotic neurons, if stained brown, show a diffuse light brown staining not only in the cell nucleus but also in the cytoplasm.

Immunohistochemical Study

Serial sections (4 μm) from frozen samples were fixed in 4% paraformaldehyde for 7 minutes at 4°C and then treated with 1% hydrogen peroxide in methanol for 30 minutes. Sections were incubated with a polyclonal rabbit anti-GFAP antibody (1:200; Z0334; DAKO, Carpinteria, Calif), which was previously treated with a peroxidase labeling kit (LK-09; Dojindo laboratories, Kumamoto, Japan), for 60 minutes at room temperature. The slices were colorized with liquid 3,3-diaminobenzidine (Liquid DAB, K3466; DAKO), and then nuclei were counterstained with hematoxylin.

For semiquantitative analysis of reactive astrogliosis, the microscopic images of the gray and white matter were captured through a charge-coupled device (CCD) camera connected to the microscope at a magnification of ×200. The obtained digital images were analyzed with a computer with image-processing software (ImageJ v1.37; National Institute of Mental Health, Bethesda, Md). The color images with various degrees of GFAP expression were converted to binary images and then to numeric data by means of particle analysis (Figure 1). The results of particle analysis represented the ratio of the accumulated area of GFAP-positive fractions over a certain size (ie, cytoplasm of astrocytes) to the whole area of the image. Those data obtained from several different sights (3 from the gray matter and 6 from the white matter) in each slice were averaged and presented as the GFAP-positive area fraction (GFAP%). The digital analyses were performed, comparing original images to binary images. The binary threshold was determined so that the signal-to-noise ratio became nearly equivalent among all images. The particle size used in particle analysis was set so that almost all astrocytes could be detected, whereas the noise could not.

Statistical Analysis

Data are expressed as the mean ± standard error of the mean. Comparison of the continuous variables was performed by using the 1-way analysis of variance test with Scheffe's multiple comparison test. Changes in the hemodynamic and blood gas analysis data over time were analyzed with repeated-measures analysis of variance. For the analysis of serial changes

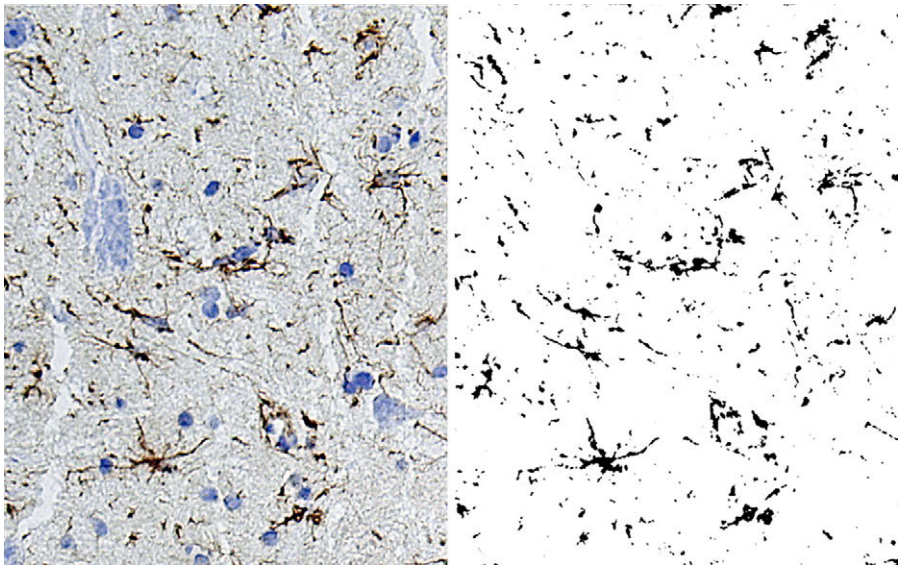

FIGURE 1. An example of conversion from a microscopic picture of a glial fibrillary acidic protein immunohistochemical stain to a binary image by using image processing software.

in Johnson scores in the same rabbits, the Friedman test was used, which was followed by the Wilcoxon signed-rank test for multiple comparison. Correlation analysis was performed with the simple linear regression test. Statistical analyses were performed with GraphPad Prism 4.0 (GraphPad Software, Inc, San Diego, Calif) and SPSS 11.0.1 for Windows (SPSS, Inc, Chicago, Ill).

RESULTS

All rabbits survived until the prescheduled time period for analyses. Table 1 demonstrated hemodynamic and blood gas analysis data during the procedure. The mean distal blood pressure decreased and the pulse pressure vanished (data not shown) after balloon inflation in all rabbits. The rectal temperature also decreased gradually during ischemia and returned to preocclusion values within 10 minutes after reperfusion. Base excess, P_{CO_2}, and blood glucose levels were significantly changed after reperfusion.

Neurologic Function

Figure 2 shows the serial change in Johnson score of 6 animals killed on the seventh day. Although hind-limb motor function was normal in 4 of 6 rabbits on the first day, it deteriorated in all rabbits thereafter. The score continued to decrease even after the third day in all rabbits, representing delayed-onset injury. A decrease in the Johnson score was statistically significant ($P < .001$) and was 4.67 ± 0.21 on the first day, 3.67 ± 0.42 on the third day ($P = .059$ vs the first day), and 2.33 ± 0.33 on the seventh day ($P = .026$ vs the first day, Figure 2).

Histologic Study

On the first day, most neurons appeared intact. On the third day, necrotic neurons were apparent, and parenchymal edema, microvascular dilatation, and leukocyte infiltration were conspicuous. On the seventh day, necrotic neurons were apparent. Parenchymal edema was significant with the loss of constructive integrity of the gray matter. Apoptotic neurons were not evident at any time period. The number of intact motor neurons in the anterior spinal cord was significantly different among the 3 time points ($P = .001$). This number was significantly smaller on the seventh day

TABLE 1. Hemodynamic and blood gas analysis data during the protocol

	Five minutes before clamping	After clamping	Before unclamping	Five minutes after unclamping
Proximal mBP (mm Hg)*	67.4 ± 2.67	79.3 ± 2.6†	73.4 ± 3.0	76.8 ± 3.5
Distal mBP (mm Hg)*	79.8 ± 2.9	12.2 ± 0.6†	14.2 ± 0.9†	87.6 ± 4.0
Rectal temperature (°C)*	39.0 ± 0.02	39.0 ± 0.02	38.5 ± 0.03†	38.9 ± 0.04
pH	7.409 ± 0.01			7.419 ± 0.01
Hematocrit (%)	37.7 ± 0.6			38.1 ± 0.7
P_{O_2} (mm Hg)	351.7 ± 14.4			342.5 ± 19.5
P_{CO_2} (mm Hg)	46.2 ± 1.7			42.9 ± 1.3‡
Base excess (mEq/L)	3.76 ± 0.84			2.87 ± 0.93‡
Glucose (g/dL)	154.6 ± 4.8			186.1 ± 7.4‡

mBP, Mean blood pressure. *$P < .05$, repeated-measures analysis of variance. †$P < .05$ compared with the value at 5 minutes before clamping, Bonferroni's multiple comparison test. ‡$P < .05$, paired *t* test.

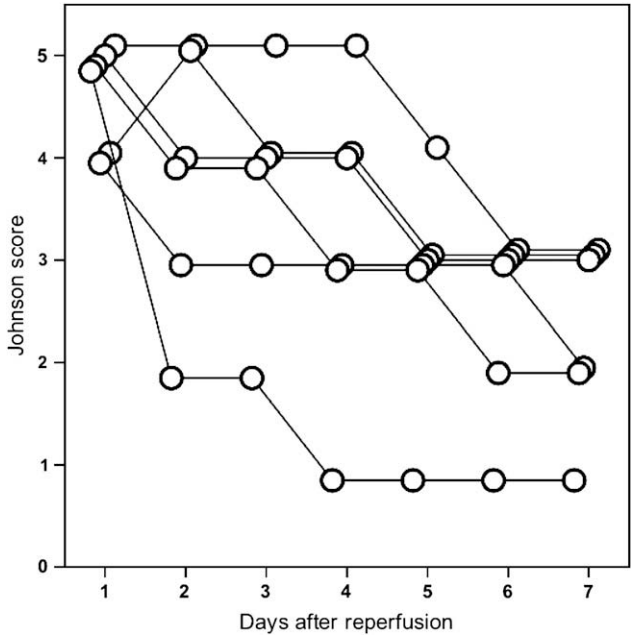

FIGURE 2. Serial change in the neurologic function graded by using Johnson's method in the 6 rabbits.

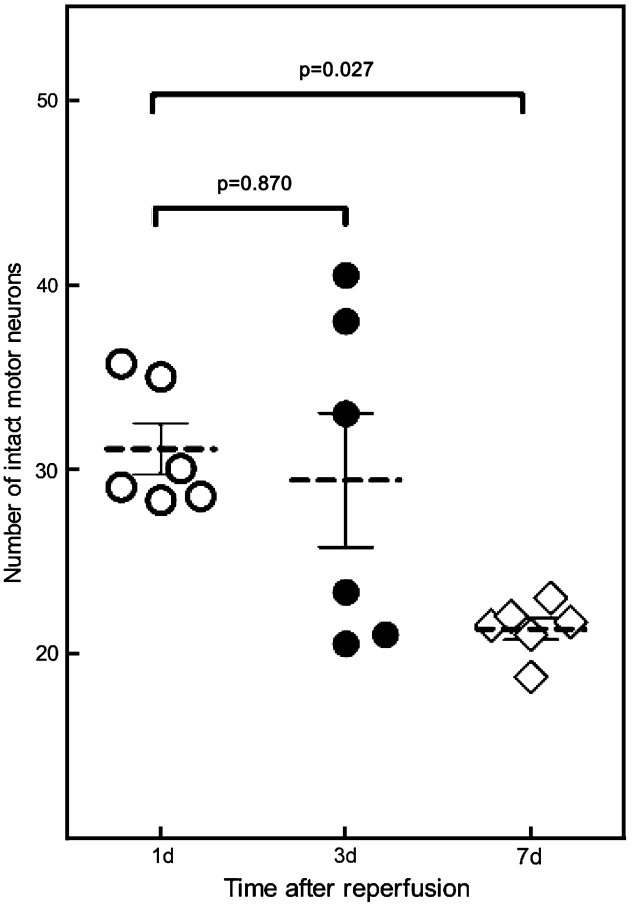

FIGURE 3. Number of intact motor neurons on the first, third, and seventh days after transient spinal cord ischemia.

(21.32 ± 0.59) than that on the first day (31.08 ± 1.37, P = .027), whereas it was comparable between the third day (29.38 ± 3.64) and the first day (P = .870). Of note, the variation of the number of intact neurons was prominent on the third day, reflecting the wide variation of Johnson scores at this time point (Figure 3). There was a significant correlation between the number of normal motor neurons and the Johnson score (r^2 = 0.658, P < .001, Figure 4). Meanwhile, no obviously TUNEL-positive motor neurons could be found at the 3 time points, although there were a few neurons presenting diffuse brown staining in both the nucleus and the cytoplasm and not being consistent with apoptotic neurons.

Immunohistochemical Study

In the gray matter reactive astrogliosis of the protoplasmic astrocytes was minimal on the first day. It became apparent on the third day around mircovessels and some motor neurons. On the seventh day, reactive astrogliosis was prominent around the damaged neurons (Figure 5, upper row). The value of GFAP% was significantly different among the 3 time points (P = .001) and was 0.47 ± 0.07 on the first day, 0.72 ± 0.09 on the third day (P = .353 vs the first day), and 1.23 ± 0.17 on the seventh day (P = .001 vs the first day and P = .025 vs the third day; Figure 6, *A*). In the white matter reactive astrogliosis of the fibrous astrocytes was already present on the first day and became prominent and seemed nearly complete on the third day (Figure 5, lower row). GFAP% was also significantly different among the 3 time points (P = .004). GFAP% on the third day (5.95 ± 0.45) was significantly higher than that on the first day

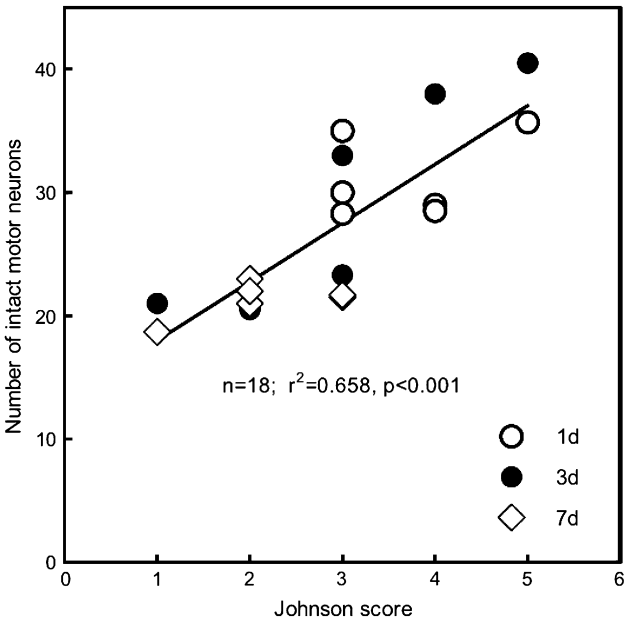

FIGURE 4. Correlation between the number of normal motor neurons and the Johnson score.

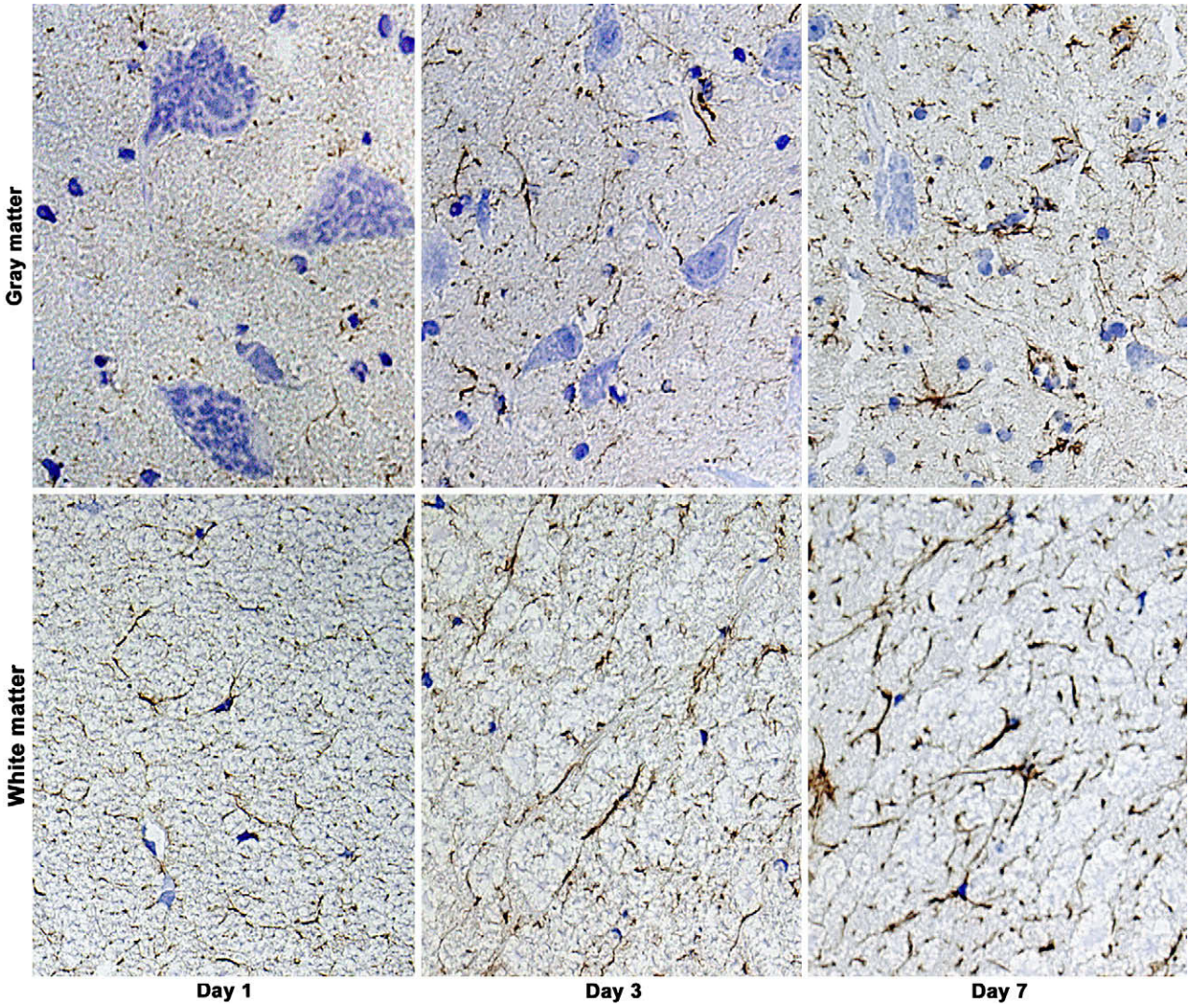

FIGURE 5. Microscopic images of immunohistochemical study for glial fibrillary acidic protein in the gray *(upper row)* and white *(lower row)* matter on the first *(left column)*, third *(middle column)*, and seventh *(right column)* days. Glial fibrillary acidic protein was stained a dense brown color.

(4.43 ± 0.27, $P = .024$), whereas that on the seventh day (6.24 ± 0.29) was not significantly different from that on the third day ($P = .841$; Figure 6, *B*). There was a significant correlation ($r^2 = 0.538$, $P < .001$) between the GFAP% values in the gray and white matter.

The linear regression analysis revealed a significant inverse correlation between GFAP% value and the number of intact neurons on the third day in both the gray ($r^2 = 0.726$, $P = .031$) and white matter ($r^2 = 0.927$, $P = .002$, Figure 7). In the gray matter a similar relationship was also observed on the first day, although it was not statistically significant ($r^2 = 0.595$, $P = .072$). On the seventh day, there was no corelationship between them.

DISCUSSION

The main observations of this study are as follows: (1) progressive and delayed deterioration of the hind-limb motor function was observed up to the seventh day after 15 minutes of spinal cord ischemia in all rabbits, with significant correlation between the Johnson neurologic score and the number of intact motor neurons; (2) development of reactive astrogliosis, which was observed in both the gray and white matter, was semiquantitatively analyzed by means of immunoreactivity for GFAP; and (3) semiquantitative analysis of the extent of GFAP expression in both the gray and white matter demonstrated significant correlation with the number of intact motor neurons on the third day.

Delayed-onset paraplegia was reported to develop 2 to 7 days after TSCI.[2-8] The group of Sakurai and associates[3] demonstrated that apoptotic motor neuron death accounted for the delayed motor dysfunction after TSCI by using TUNEL staining and immunohistochemical study for caspase-3[4] and Fas antigen[5] expression. Matsumoto and colleagues,

CPS

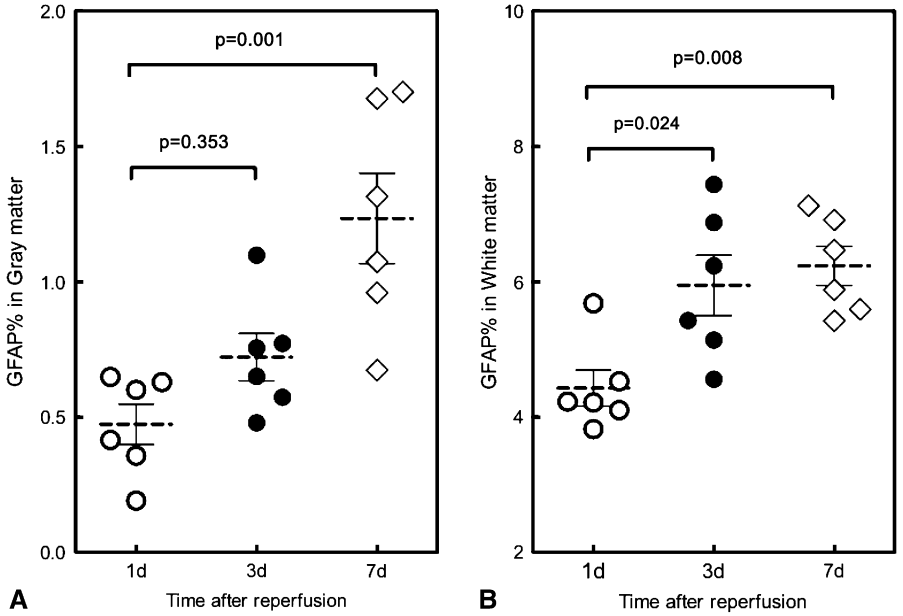

FIGURE 6. Glial fibrillary acidic protein immunoreactivity *(GFAP%)* on the first, third, and seventh days after transient spinal cord ischemia in the gray (A) and white (B) matter.

however, suggested that delayed motor neuron death was predominantly associated with necrotic death[7] and could develop if the ischemic insult exceeds the protection by astrocytes because astrocytes were considered to be activated by ischemia and to protect neurons.[8] Our result that there were no obvious TUNEL-positive motor neurons was in accordance with the Matsumoto reports. However, we cannot exclude apoptotic neuronal death as a mechanism of delayed injury because other reliable assays, such as immunohistochemical study for cleaved caspase-3 or cleaved poly–adenosine diphosphate–ribose polymerase, were not performed. Further study will be necessary in this regard.

The inverse correlation between the extent of GFAP expression and the number of intact motor neurons observed on the third day might suggest that reactive astrocytes play an important role in the delayed motor neuron death. Alternatively, reactive gliosis was caused by neuronal injury, which was the reason for this correlation. However, the correlation with the number of intact neurons was present not only for the GFAP% in the gray matter but also for that in the white matter, and GFAP% in the white matter was in parallel with that in the gray matter. These results suggest that astrocytes activation was triggered globally by the initial ischemic event, rather than triggered locally by damaged neurons. In addition, if gliosis is merely a response to

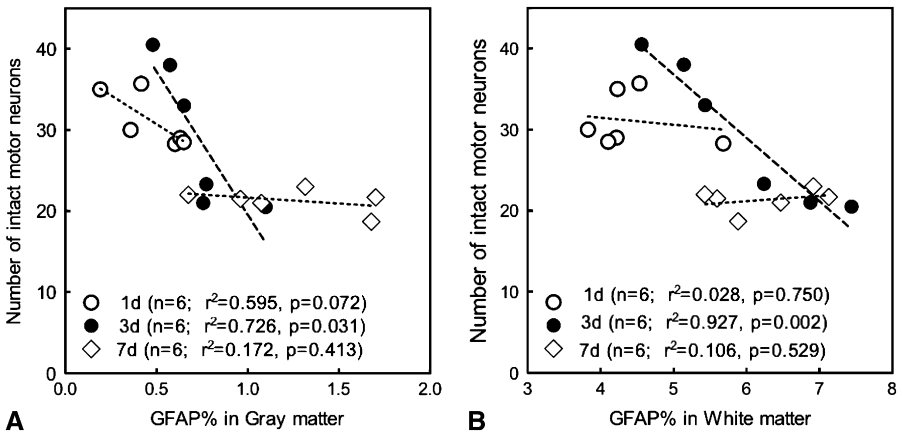

FIGURE 7. Linear regression analysis for the correlation between the number of intact motor neurons and glial fibrillary acidic protein *(GFAP)* immunoreactivity on the first, third, and seventh days after transient spinal cord ischemia in the gray (A) and white (B) matter.

cellular death, such correlation should also be significant on the seventh day, when neuronal death was more prominent. Together with the localization of reactive astrocytes surrounding damaged neurons, we think that reactive astrocytes are involved in the mechanism of delayed motor neuron death.

Reactive astrocytes are characterized by hypertrophy of cellular processes and upregulation of GFAP and vimentin.[15] GFAP is a chief component of intermediate filaments, which, together with microtubules and actin filaments, constitute the cytoskeleton of astrocytes. The protoplasmic astrocytes in the gray matter were reported to have smaller amounts of GFAP than the fibrous astrocytes in the white matter,[16] which could explain the more rapid expression of GFAP in the white matter in our study. Upregulation of GFAP is perhaps the best known hallmark of reactive astrocytes and reactive gliosis. Within a few hours of virtually any type of brain injury, surviving astrocytes in the affected region begin to exhibit hypertrophy and proliferation.[17] GFAP immunoreactivity becomes strongly positive at 48 to 72 hours after reperfusion,[8,11,12] which persists in damaged areas for weeks after ischemia, without conspicuous cell loss.[18] Our results on semiquantitative analysis were consistent with these reports.

The functions of astrocytes are numerous and complex. Astrocytes are sensors of changes in the brain environment, to which they immediately react on the genomic (eg, production of trophic factors) and nongenomic (eg, uptake of ions) levels.[19,20] Astrocytes are sources of energy substrates for neurons. They transfer lactate, pyruvate, or both to neurons[21] and store glycogen as the main energy reserve in the brain.[22] There were numerous reports suggesting that reactive astrocytes could be closely associated with neuronal survival after ischemia. Muyderman and coworkers[23] reported that selective depletion of mitochondrial glutathione in astrocytes increased the sensitivity to peroxynitrate and was associated with necrotic cell death. Li and colleagues[24] demonstrated the neuroprotective role of reactive astrocytes in brain ischemia. Excitatory glutamatergic neurotransmission is controlled by astrocytes on biosynthesis and uptake of glutamate,[25] consequently preventing neuronal death caused by excitotoxicity.[26] Under pathologic conditions (eg, hypoxemia), however, astrocytes could release exocytotic glutamate through glutamate transporters.[27,28] Hence activated astrocytes might both protect against and contribute to the glutamate-mediated neuronal damage.

In this study we introduced a new method for semiquantitative analysis of GFAP expression and, by using it, successfully demonstrated the correlation between the number of intact motor neurons and GFAP expression. Although the decision of binary threshold or particle size and adjustment of signal-to-noise ratio are relatively a delicate matter, the particle analysis of digitized photographic data is simple, cost-effective, and highly reproducible compared with traditional procedures, such as histologic grading/scoring. It requires no fluorescent staining and special equipment like fluorescence microscopy. We could perform histologic analysis and semiquantitative immunologic analysis simultaneously and could even compare them by using single-sample slides. The present report will open a new window for further research into ischemic spinal cord injury.

References

1. Cambria RP, Davison JK, Carter C, Brewster DC, Chang Y, Clark KA, et al. Epidural cooling for spinal cord protection during thoracoabdominal aneurysm repair: a five-year experience. *J Vasc Surg*. 2000;31:1093-102.
2. Moore WMJ, Hollier LH. The influence of severity of spinal cord ischemia in the etiology of delayed-onset paraplegia. *Ann Surg*. 1991;213:427-32.
3. Sakurai M, Hayashi T, Abe K, Sadahiro M, Tabayashi K. Delayed and selective motor neuron death after transient spinal cord ischemia: a role of apoptosis? *J Thorac Cardiovasc Surg*. 1998;115:1310-5.
4. Hayashi T, Sakurai M, Abe K, Sadahiro M, Tabayashi K, Itoyama Y. Apoptosis of motor neurons with induction of caspases in the spinal cord after ischemia. *Stroke*. 1998;29:1007-13.
5. Sakurai M, Hayashi T, Abe K, Sadahiro M, Tabayashi K. Delayed selective motor neuron death and fas antigen induction after spinal cord ischemia in rabbits. *Brain Res*. 1998;797:23-8.
6. Sakurai M, Nagata T, Abe K, Horinouchi T, Itoyama Y, Tabayashi K. Oxidative damage and reduction of redox factor-1 expression after transient spinal cord ischemia in rabbits. *J Vasc Surg*. 2003;37:446-52.
7. Kiyoshima T, Fukuda S, Matsumoto M, Iida Y, Oka S, Nakakimura K, et al. Lack of evidence for apoptosis as a cause of delayed onset paraplegia after spinal cord ischemia in rabbits. *Anesth Analg*. 2003;96:839-46.
8. Matsumoto S, Matsumoto M, Yamashita A, Ohtake K, Ishida K, Morimoto Y, et al. The temporal profile of the reaction of microglia, astrocytes, and macrophages in the delayed onset paraplegia after transient spinal cord ischemia in rabbits. *Anesth Analg*. 2003;96:1777-84.
9. Anderson MF, Blomstrand F, Blomstrand C, Eriksson PS, Nilsson M. Astrocytes and stroke: networking for survival? *Neurochem Res*. 2003;28:293-305.
10. Swanson RA, Ying W, Kauppinen TM. Astrocyte influences on ischemic neuronal death. *Curr Mol Med*. 2004;4:193-205.
11. Matsui T, Mori T, Tateishi N, Kagamiishi Y, Satoh S, Katsube N, et al. Astrocytic activation and delayed infarct expansion after permanent focal ischemia in rats. Part I: enhanced astrocytic synthesis of s-100beta in the periinfarct area precedes delayed infarct expansion. *J Cereb Blood Flow Metab*. 2002;22:711-22.
12. Yasuda Y, Tateishi N, Shimoda T, Satoh S, Ogitani E, Fujita S. Relationship between S100beta and GFAP expression in astrocytes during infarction and glial scar formation after mild transient ischemia. *Brain Res*. 2004;1021:20-31.
13. Wakamatsu Y, Shiiya N, Kunihara T, Watanabe S, Yasuda K. The adenosine triphosphate-sensitive potassium channel opener nicorandil protects the ischemic rabbit spinal cord. *J Thorac Cardiovasc Surg*. 2001;122:728-33.
14. Johnson SH, Kraimer JM, Graeber GM. Effects of flunarizine on neurological recovery and spinal cord blood flow in experimental spinal cord ischemia in rabbits. *Stroke*. 1993;24:1547-53.
15. Pekny M, Nilsson M. Astrocyte activation and reactive gliosis. *Glia*. 2005;50:427-34.
16. Walz W. Controversy surrounding the existence of discrete functional classes of astrocytes in adult gray matter. *Glia*. 2000;31:95-103.
17. Ridet JL, Malhotra SK, Privat A, Gage FH. Reactive astrocytes: cellular and molecular cues to biological function. *Trends Neurosci*. 1997;20:570-7.
18. Petito CK, Morgello S, Felix JC, Lesser ML. The two patterns of reactive astrocytosis in postischemic rat brain. *J Cereb Blood Flow Metab*. 1990;10:850-9.
19. Trendelenburg G, Dirnagl U. Neuroprotective role of astrocytes in cerebral ischemia: focus on ischemic preconditioning. *Glia*. 2005;50:307-20.
20. Leis JA, Bekar LK, Walz W. Potassium homeostasis in the ischemic brain. *Glia*. 2005;50:407-16.
21. Forsyth RJ. Astrocytes and the delivery of glucose from plasma to neurons. *Neurochem Int*. 1996;28:231-41.
22. Dringen R, Gebhardt R, Hamprecht B. Glycogen in astrocytes: possible function as lactate supply for neighboring cells. *Brain Res*. 1993;623:208-14.

23. Muyderman H, Nilsson M, Sims NR. Highly selective and prolonged depletion of mitochondrial glutathione in astrocytes markedly increases sensitivity to peroxynitrite. *J Neurosci*. 2004;24:8019-28.
24. Li L, Lundkvist A, Andersson D, Wilhelmsson U, Nagai N, Pardo AC, et al. Protective role of reactive astrocytes in brain ischemia. *J Cereb Blood Flow Metab*. 2008;28:468-81.
25. Hertz L, Zielke HR. Astrocytic control of glutamatergic activity: astrocytes as stars of the show. *Trends Neurosci*. 2004;27:735-43.
26. Anderson CM, Swanson RA. Astrocyte glutamate transport: review of properties, regulation, and physiological functions. *Glia*. 2000;32:1-14.
27. Takahashi M, Billups B, Rossi D, Sarantis M, Hamann M, Attwell D. The role of glutamate transporters in glutamate homeostasis in the brain. *J Exp Biol*. 1997; 200:401-9.
28. Parpura V, Scemes E, Spray DC. Mechanisms of glutamate release from astrocytes: gap junction ''hemichannels,'' purinergic receptors and exocytotic release. *Neurochem Int*. 2004;45:259-64.

CPS